Strong-motion parameters of the M_w=6.3 Abruzzo (Central Italy) earthquake.

By
Ameri G., Augliera P., Bindi D., D'Alema E., Ladina C., Lovati S., Luzi L., Marzorati S., Massa M., Pacor F.

1. Introduction

On April 6, 2009 at 01:32:39 GMT a magnitude Mw=6.3 (Harvard CMT) earthquake occurred in the Abruzzo region (Central Italy), close to the town of L'Aquila (located at about 6 km northeast to the epicenter). The mainshock has been recorded by 55 stations belonging to the Italian Strong Motion Network (RAN managed by the Italian Department of Civil Protection, DPC) (http://www.protezionecivile.it/minisite/index.php?dir_pk=1036&cms_pk=15425). Soon after the earthquake occurred the first emergency structures of the National Earthquake Centre of INGV (*Struttura di Pronto Intervento, SPI*) was activated, to install in the epicentral area the stations of the real-time temporary seismic network. In addition several institutions, such as the Istituto Nazionale di Geofisica e Vulcanologia (INGV), the University of Potenza and the Helmholtz-Zentrum Potsdam (Deutsches GeoForschungsZentrum – GFZ) installed about 30 stations to detect site effects and the response of buildings. In Figure 1 the RAN stations installed in the epicentral area are shown. This event is the third largest earthquake recorded by strong-motion instruments since 1972, after the 1976 Friuli (Mw=6.4) and the 1980 Irpinia (Mw=6.9).
In this note we present the strong motion parameters of engineering interest computed for the mainshock, recorded by the stations of the RAN.

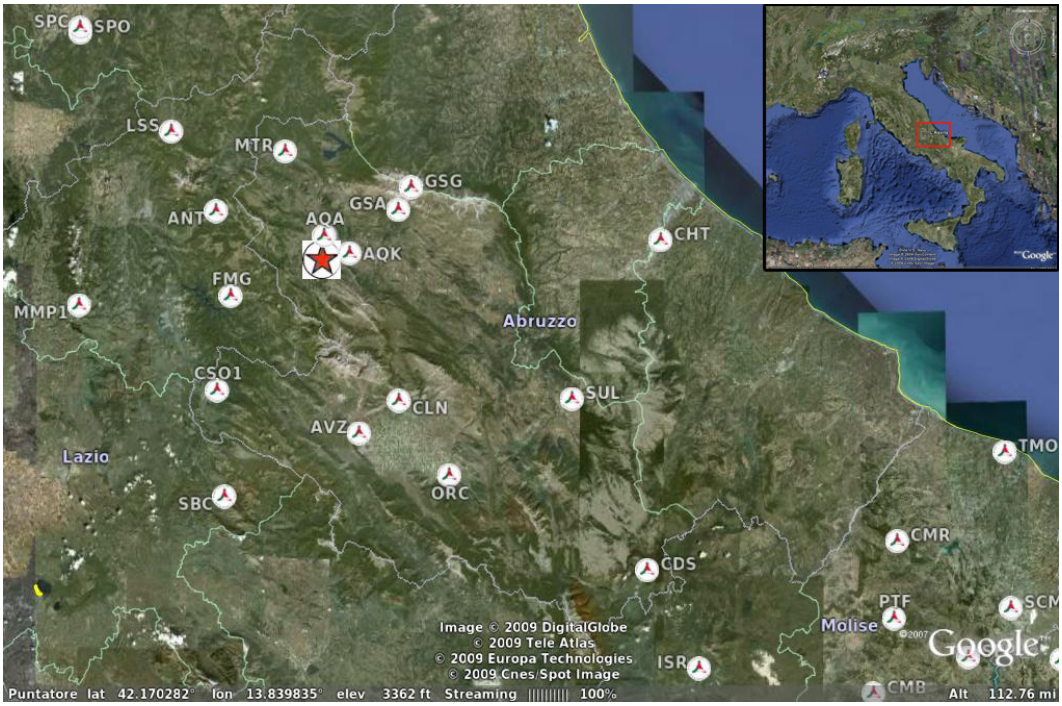

Figure 1- Distribution of the RAN seismic stations installed in the epicentral area. The epicenter is shown as a red star.

2. Events and historical seismicity

The April 6, 2009 Abruzzo earthquake has been generated by a normal fault, with NW-SE trend and SW dip. The strongest aftershocks occurred on April 7 at 17:47:37 (Mw = 5.5), located south-east to the mainshock (Figure 2), and on April 9 at 00:52:59 (Mw = 5.4) in the *Monti della Laga* area, located north to the mainshock. The hypocentral coordinates and the main parameters of the strongest events are shown in Table 1, where the focal solution is shown as well.

Table 1- Main events of the sequence

ID	Date	OT	Lat[(1)]	Lon[(1)]	depth[(1)]	Ml[(1)]	Mw*	strike;dip;rake*
2206550980	09/04/2009	19:38:16	42.501	13.356	17.2	4.9	5.2	123, 53, -110
2206541910	09/04/2009	04:32:44	42.445	13.42	8.1	4		
2206539720	09/04/2009	00:52:59	42.484	13.343	15.4	5.1	5.4	130, 48, -112
1206521070	07/04/2009	17:47:37	42.275	13.464	15.1	5.3	5.5	106, 51, -138
2206516040	07/04/2009	09:26:28	42.342	13.388	10.2	4.7		
2206509940	06/04/2009	23:15:37	42.451	13.364	8.6	4.8		
2206505980	06/04/2009	16:38:09	42.362	13.333	10.2	4		
2206497570	06/04/2009	02:37:04	42.366	13.34	10.1	4.6		
2206496920	06/04/2009	01:32:39	42.334	13.334	8.8	5.8	6.3	127, 50, -109

(1) Istituto Nazionale di Geofisica e Vulcanologia
*Harvard CMT

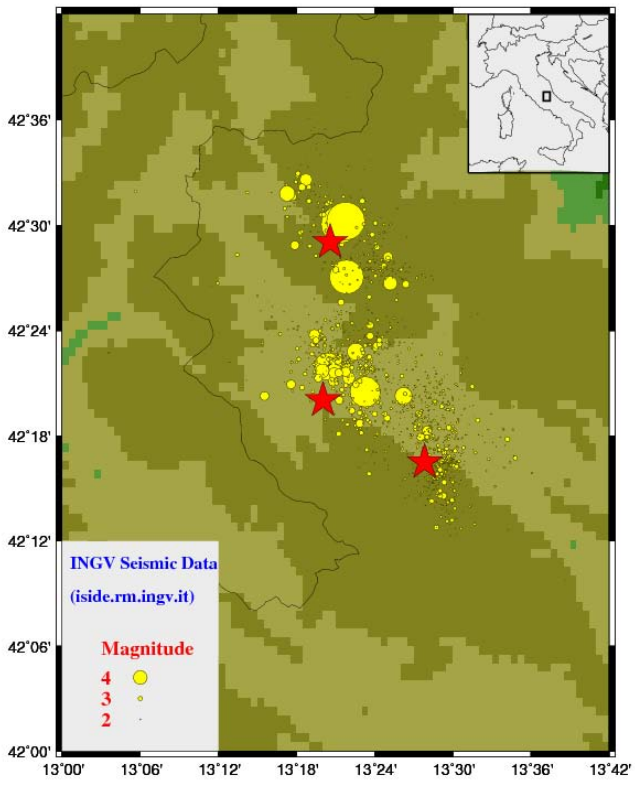

Figure 2- Mainshock and aftershocks of the L'Aquila sequence.

This area has been struck by destructive earthquakes in the past documented since 1300 BC (Stucchi et al., 2007). The three strongest earthquakes occurred in 1349 (epicentral intensity I_0=IX-X MCS), 1461(I_0=X) and 1703 (I_0=X). The historical seismicity of L'Aquila is shown in Figure 3. In particular, the 26 November 1461 event presents an epicenter location and a distribution of the most damaged sites (Figure 4) comparable to the observed damage after the L'Aquila mainshock.

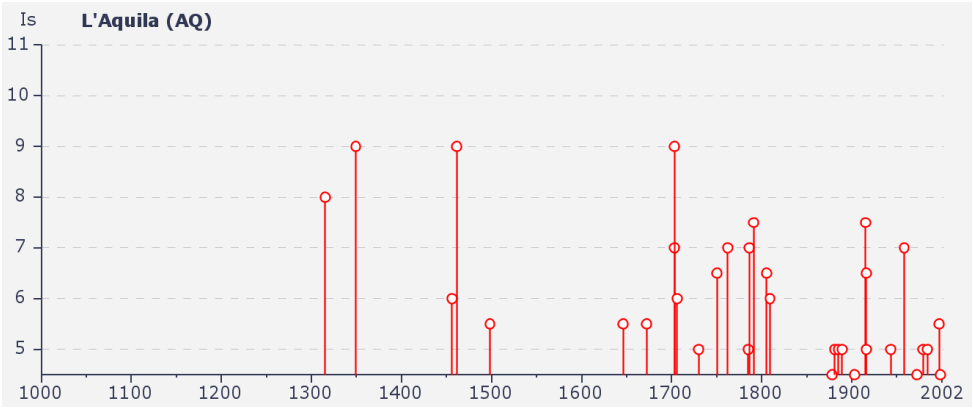

Figure3- Historical seismicity of L'Aquila. (Stucchi et al., 2007)

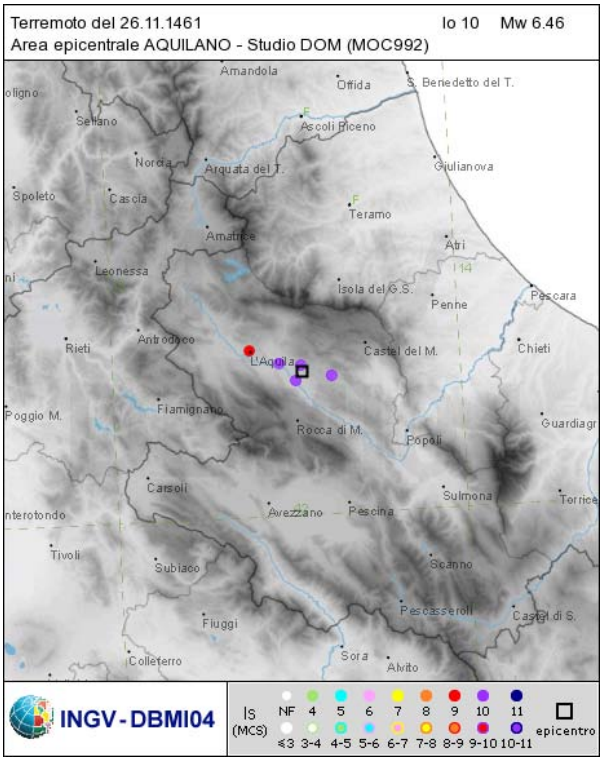

Figure 4 - 1461 earthquake intensity data (Stucchi et al., 2007)

3. Recording stations

The mainshock has been recorded by 55 stations of the Italian strong motion network (RAN).
Table 2 lists the main characteristics of the recording stations. Two site classifications are proposed. The first is the one adopted by Sabetta and Pugliese (1987, 1996) where 3 classes are discriminated on the base of shear wave velocity and depth (0 = rock sites, 1 = deposits with depth less than 20 m; 2 = deposits with depth larger than 20m) and the second is the EC8 classification derived from geological/geophysical information (project S4, http://esse4.mi.ingv.it). In particular, the classes denoted with star have been attributed on the basis of a direct measure of the Vs30. Most of the stations belong to class A or B, while few stations belong to class C.

Table 2 - RAN Stations

Code	Name	lat	Lon	class_SP	class_EC8
ANT	ANTRODOCO	42.418	13.079	0	A
AQA	L'AQUILA - V. ATERNO -F. ATERNO	42.376	13.339	1	B
AQG	L'AQUILA - V. ATERNO -COLLE GRILLI	42.373	13.337	1	B
AQK	AQUIL PARK ING.	42.345	13.401	2	C
AQV	L'AQUILA - V. ATERNO - CENTRO VALLE	42.377	13.344	2*	B*
ASS	ASSISI	43.075	12.604	0	A
AVL	AVELLINO	40.923	14.787	1	B
AVZ	AVEZZANO	42.027	13.426	2	C
BBN	BIBBIENA	43.748	11.821	2	C
BDT	BADIA TEDALDA	43.707	12.188	0	A
BNE	BENEVENTO	41.128	14.785	1	B
BOJ	BOJANO	41.484	14.472	2	C
CDS	CASTEL DI SANGRO	41.787	14.112	0	A
CER	CERIGNOLA	41.26	15.91		
CHT	CHIETI	42.37	14.148	2	C
CLN	CELANO	42.085	13.521	0	A
CMB	CAMPOBASSO	41.563	14.652	0	A
CMR	CASTELMAURO	41.833	14.712		
CNM	CASALNUOVO MONTEROTARO	41.618	15.105	0	A
CSO1	CARSOLI 1	42.101	13.088	0	A
CSS	CASSINO	41.486	13.823	0	A
CTL	CATTOLICA	43.955	12.736		
FMG	FIAMIGNANO	42.268	13.117	0	A
FOR	FORLI'	44.199	12.042	2	C
GNL	GENZANO DI LUCANIA	40.843	16.033	0	A
GSA	GRAN SASSO (ASSERGI)	42.421	13.519	0	A
GSG	GRAN SASSO (LAB. INFN GALLERIA)	42.46	13.55	0	A
ISR	ISERNIA	41.611	14.236	1	B
LSS	LEONESSA	42.558	12.969	0	A
MMP1	MOMPEO 1	42.249	12.748	0	A
MNG	MONTE S. ANGELO	41.704	15.958		
MNN	MANFREDONIA	41.634	15.911	0	A
MTR	MONTEREALE	42.524	13.245	2	A
NAP	NAPOLI OVEST	40.799	14.18	2	C
ORC	ORTUCCHIO	41.954	13.642	0	A
PDM	PIEDIMONTE MATESE	41.355	14.385	2	C

Code	Name	lat	Lon	class_SP	class_EC8
PIC	PIANCASTAGNAIO	42.85	11.685	1	B
PTF	PETRELLA TIFERNINA	41.696	14.702		
RIC	RICCIA	41.483	14.838	0	A
SBC	SUBIACO	41.913	13.106	0	A
SCM	S. CROCE DI MAGLIANO	41.711	14.984	1	B
SCP	SERRACAPRIOLA	41.807	15.165		
SDG	S. GIOVANNI ROTONDO	41.709	15.733		
SEP	S. ELIA A PIANISI	41.625	14.88	0	A
SNM	SAN MARINO	43.934	12.449	0	A
SNS	SANZA	40.243	15.55	0	A
SPC	SPOLETO (CANTINA)	42.743	12.74	2	C
SPO	SPOLETO	42.734	12.741	0	A
SSR	S. SEVERO	41.691	15.374	2	C
STN	STURNO	41.018	15.112	0	A
SUL	SULMONA	42.089	13.934	0	A
TLS	TELESE TERME	41.222	14.53	0	A
TMO	TERMOLI	41.989	14.975		
VIE	VIESTE	41.877	16.165		
VRP	VAIRANO PATENORA	41.333	14.132	1	B

4. The strong motion records of the mainshock

The mainshock strong-motion data have been recorded at epicentral distances ranging from 4 to 297 km and Joyner-Boore distances (R_{jb}) ranging from 0 to 284 km (in the following we will assign, for graphic reasons, R_{jb}=1 to sites formally having R_{jb}=0). In particular, 23 records at distances smaller than 50 km are available. To compute the R_{jb} distance, the geometry of the fault has been hypothesized by merging different information, such as geology, distribution of the aftershocks and geodetic observations (Figure 5).

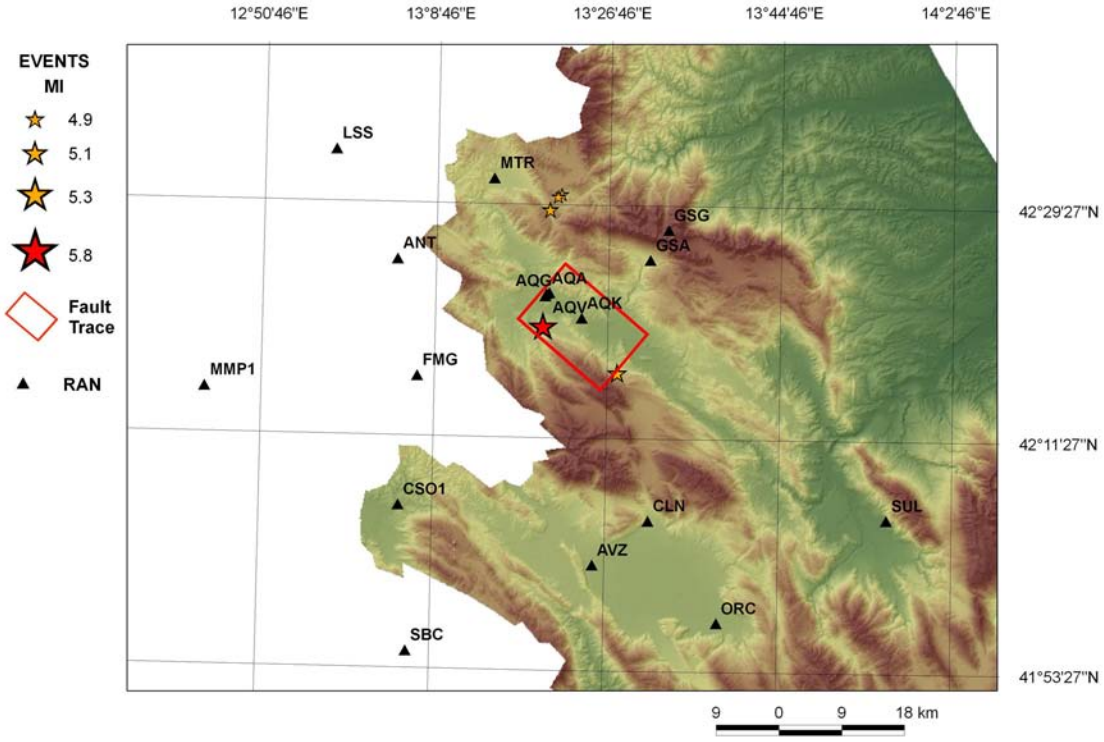

Figure 5 - Fault geometry plotted against the main events. Triangles show the RAN seismic stations installed in the epicentral area.

In Table 3 the main parameters for each strong motion record (epicentral and Joyner-Boore distances, maximum horizontal PGA and maximum horizontal PGV) are listed.
The observed largest PGA (PGV) is 646 cm/s^2 (43 cm/s) recorded at station *Valle dell'Aterno – Centro Valle* (AQV), but, in general all the near fault PGA are larger than 350 cm/s^2 and the PGV are larger than 30 cm/s.
Figure 6 shows the EW component of the acceleration time series recorded by the closest stations to the epicenter (AQK, AQA, AQV and AQG). Near-source long-period pulses, possibly related to source effects, are present in all the records. However the effect of the site response, discussed in paragraph 7, is visible in L'Aquila (AQK) record which shows the highest low frequency content and in the AQA record, which exhibits a high-frequency content.

Table 3 - Peak ground acceleration and velocity recorded at each RAN station (maximum between the horizontal components)

Code	R_{jb} (km)	R_{epi} (km)	Max H PGA (cm/s^2)	Max H PGV (cm/s)
ANT	19.3	23.0	25.98	2.47
AQA	0.1	4.6	435.63	32.03
AQG	0.1	4.4	506.86	35.54
AQK	0.1	5.6	347.23	36.21
AQV	0.1	4.9	646.07	42.83
ASS	96.5	101.7	6.04	0.43
AVL	185.7	198.0	1.25	0.38
AVZ	25.1	34.9	67.68	11.28
BBN	194.5	199.5	1.00	0.24
BDT	172.8	178.8	1.99	0.38
BNE	167.9	180.2	2.06	0.68
BOJ	121.1	133.4	14.16	3.33
CAN	217.6	217.6	1.86	0.33
CDS	76.2	88.4	9.95	1.72
CHT	52.2	67.0	29.41	7.91
CLN	20.0	31.6	89.14	6.64
CMB	126.5	138.7	2.88	1.30
CMR	112.9	126.6	5.34	0.74
CNM	153.1	166.6	1.88	0.84
CSO1	31.7	33.5	18.28	2.29
CSS	91.1	102.6	9.44	1.64
CTL	178.8	186.7	4.37	0.76
FMG	16.6	19.3	26.34	2.61
FOR	225.6	232.3	1.58	0.63
GNL	266.5	279.0	2.19	0.57
GSA	8.6	18.0	148.22	9.84
GSG	13.7	22.6	29.43	3.04
ISR	97.3	109.7	7.21	0.78
LSS	35.6	39.0	9.64	0.83
MMP1	45.9	49.1	8.83	0.89
MNN	212.4	226.8	2.38	3.53
MTR	15.9	22.4	61.58	0.83
NAP	173.1	184.6	2.65	5.86
ORC	37.3	49.3	64.23	5.86
PDM	127.1	139.4	1.54	0.30
PIC	143.0	146.7	1.24	0.30
PTF	120.4	133.4	6.86	1.31
RIC	144.1	156.3	2.54	0.56
SBC	46.6	50.4	6.64	1.26
SCM	139.2	152.9	4.32	0.80
SCP	147.8	162.1	5.65	1.19
SDG	195.6	191.6	1.33	0.20
SEP	137.1	150.2	3.67	0.83
SNM	184.7	191.9	2.29	0.70
SNS	284.9	167.9	3.82	0.74
SPC	63.2	66.7	7.55	0.69
SPO	62.6	65.9	9.57	0.81
SSR	169.0	183.1	5.33	1.25
STL	277.0	277.0	0.94	0.27
STN	195.6	207.8	1.32	0.29
SUL	43.4	56.4	33.64	3.73
TLS	146.2	158.5	2.59	0.56
TMO	126.0	140.6	9.84	2.88
VIE	224.2	239.0	2.21	0.48
VRP	117.5	129.4	3.53	0.81

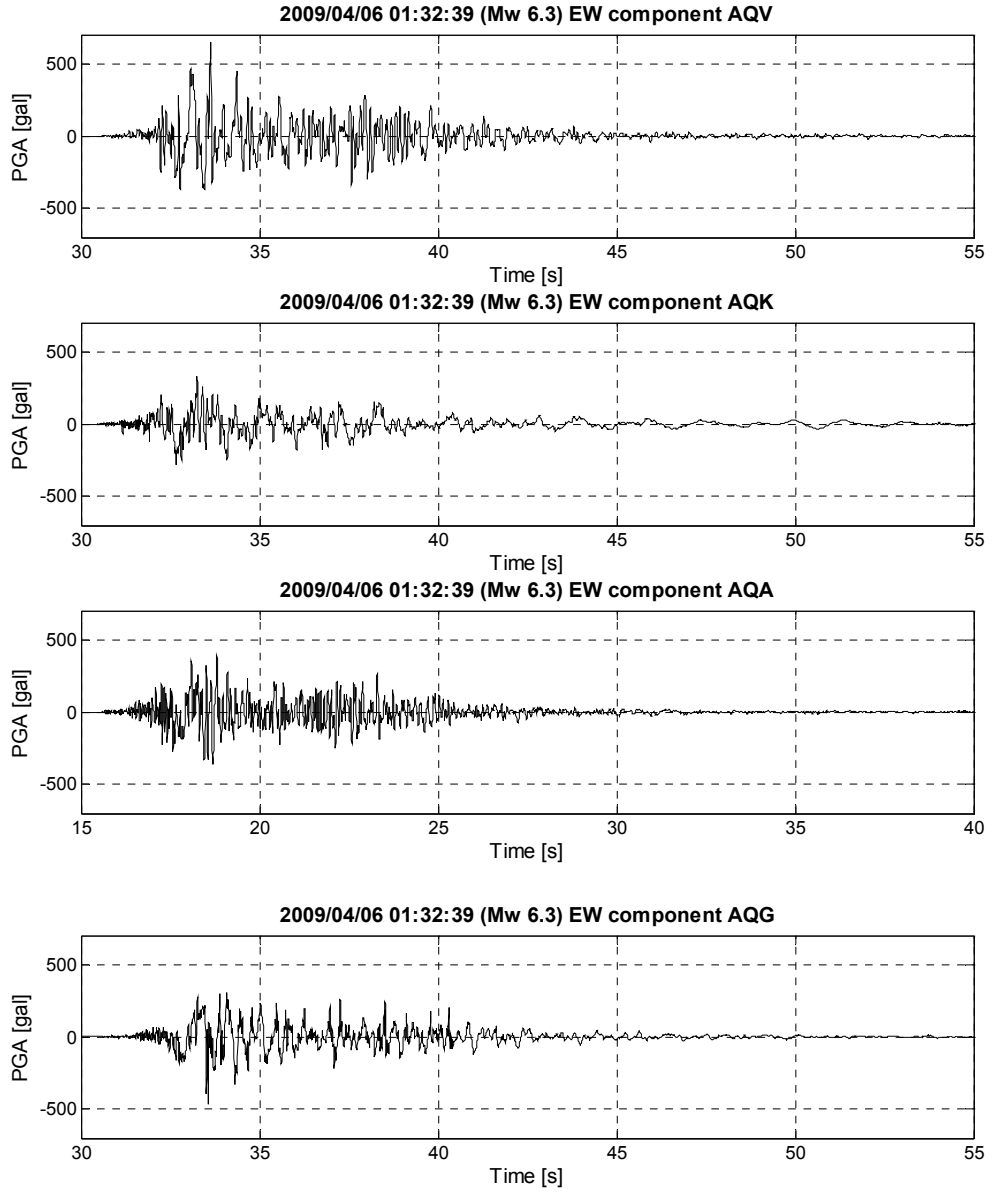

Figure 6 - EW component of the acceleration time series recorded by the stations located within 6 km from the epicenter.

5. Comparison with predictive models

Corrected data have been obtained by a standard processing (non standard errors removal, baseline correction, band pass filtering with acasual filter selected by visual inspection, integration of the corrected acceleration in order to obtain velocity). The peak ground motions calculated from processed data have been compared with the prediction obtained using different ground motion prediction equations (GMPEs): Sabetta and Pugliese (1996, SP96), Bindi et al. (2008, ITA08), Ambraseys et al. (2005, AM05), Faccioli and Cauzzi (2008, FC08) and Akkar and Bommer (2007, AkBo07). Note that ITA08 and SP96 GMPEs are calculated using data from Italian earthquakes only. In the

following (unless otherwise noted) we will plot the ground motion estimated from GMPEs in terms of mean ± one standard deviation.
Figure 7 shows the comparison with ITA08 and SP96 both for the maximum horizontal and vertical components.
In general, ITA08 underestimates the peak acceleration of sites located within the surface projection of the fault (R_{jb} = 0.0 km) by about a factor of 2, while Sabetta and Pugliese (1996) does not. Both overestimate the acceleration for distances larger than 20 km. A better fit is obtained for the peak ground velocity, especially for the vertical component.

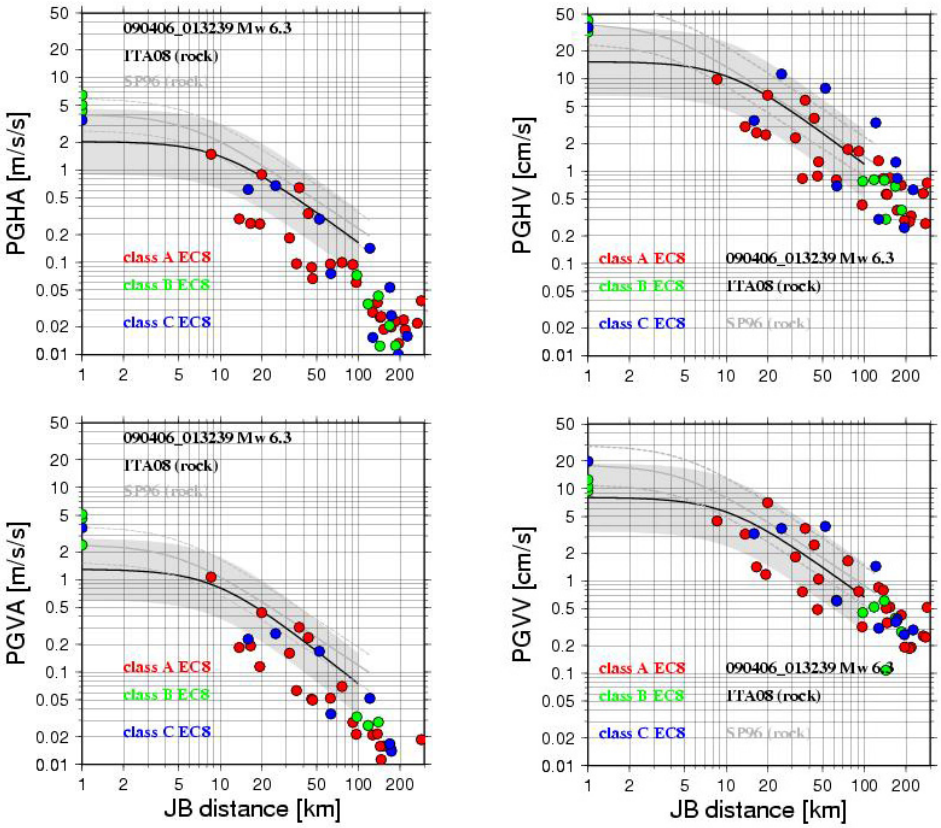

Figure 7 - Left: recorded PGAs for different site classes plotted as a function of the R_{jb} distance compared with the ITA08 and SP96 median ± one standard deviation curves for rock sites and for maximum horizontal component (Top) and vertical component (Bottom). Right: the same as left figures but for PGV.

As a preliminary investigation of the possible causes of the peak parameters overestimation, the stations (for R_{jb} < 100km) are subdivided by their azimuth from the epicentre in order to look for potential asymmetries in the ground motion distribution. In Figure 8 we compare ITA08 with observations divided into two azimuth classes. Red dots indicate stations having azimuth from 0° to 180° (located eastward to the epicenter), while blue dots span the remaining azimuths (sites located westward to the epicenter). It can be noticed how almost all the sites with azimuth from 180° to 360° are overestimated.

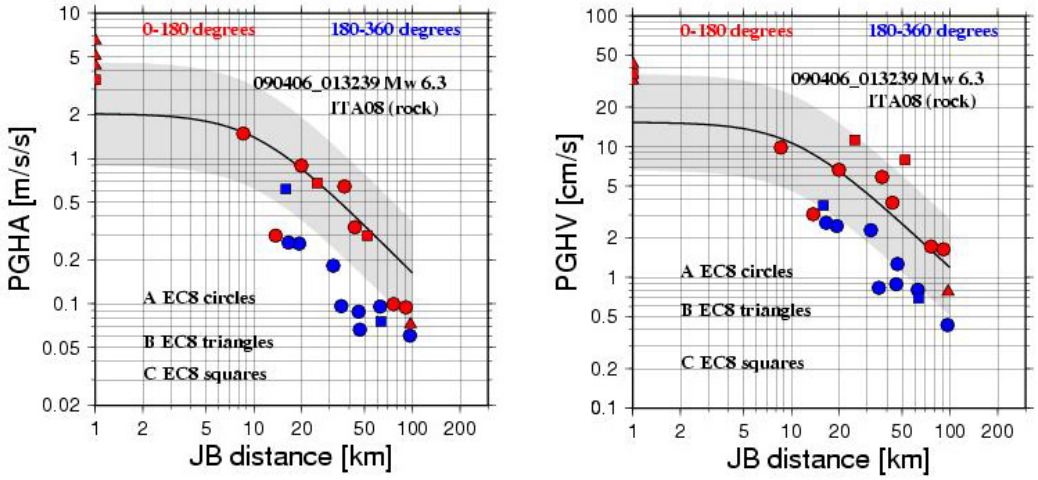

Figure 8- ITA08 curves for rock site compared with observed values divided into two azimuth classes. Red symbols indicate sites located at azimuths between 0 and 180°, blue symbols sites with azimuths between 180° and 360°

In Figure 9, the acceleration response spectra for horizontal (RSHA) and vertical (RSVA) components (at 5% damping), observed at two different stations (AQG – class B and GSA – Class A) are compared with the ITA08 predictions. A fairly good fit is observed at both stations although ITA08 underestimates the spectra recorded at AQG station at long periods.

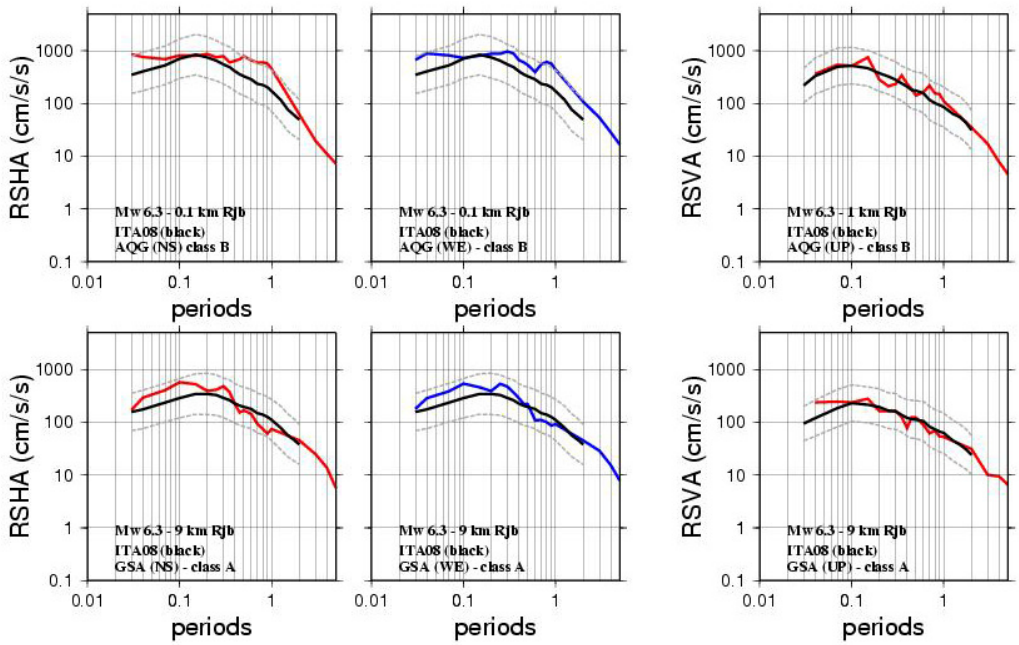

Figure 9 - Observed response spectra at two stations compared with ITA08 predictions.

Figures 10 and 11 show the comparisons with other ground motion prediction equations based on European (Ambraseys, 2005; Akkar and Bommer, 2007) and worldwide (Cauzzi and Faccioli, 2008) strong motion records. In general, all the predictive models overestimate the PGA recorded at distances larger than 30 km, while a better fit is found for PGV.

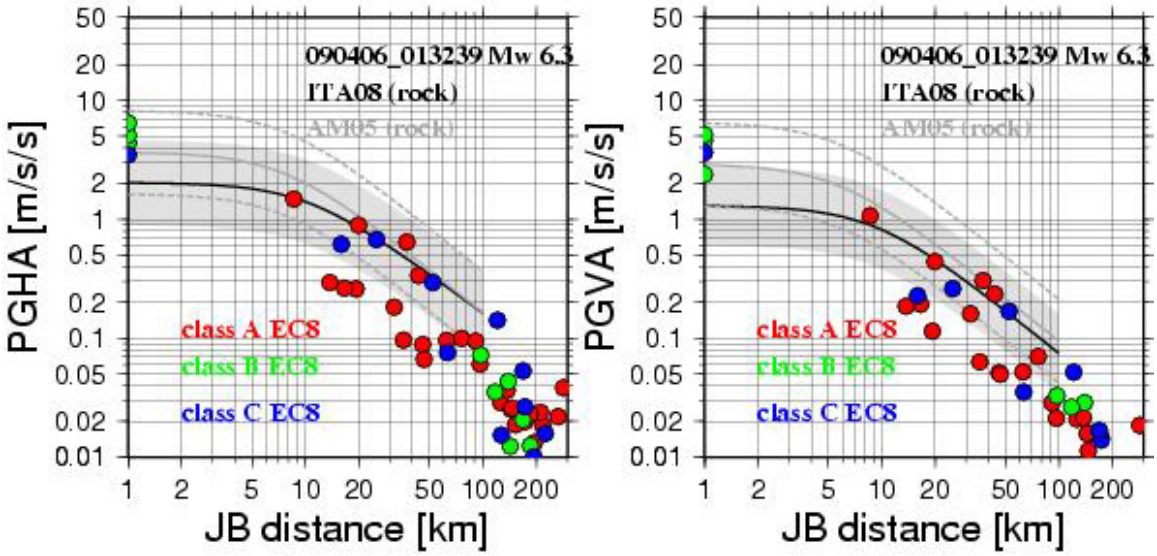

Figure 10 - Comparison between observed data and AM05 predictions (rock sites) for Horizontal (left) and vertical (right) maximum horizontal PGA. ITA08 curves are also shown.

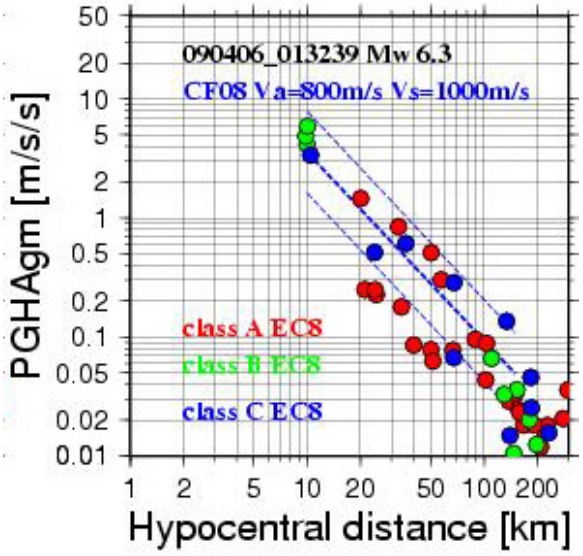

Figure 11 - Comparison between observed data and CF08 predictions (rock sites, Vs30=1000m/s) for hypocentral distance and for geometric mean of horizontal PGAs.

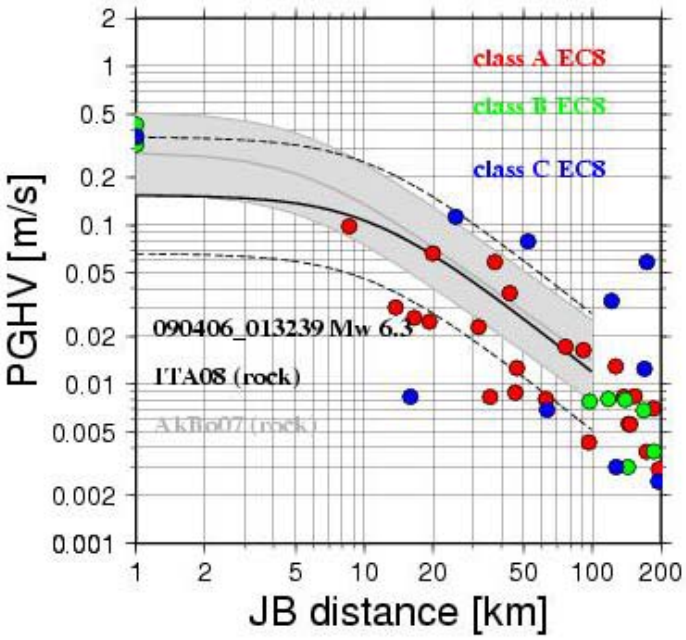

Figure 12 - comparison between observed data and the AkBo07 predictions (rock sites) for maximum horizontal PGV. ITA08 curves are also shown.

6. Comparison with EC8

In Figure 13 the 5% damped acceleration response spectra for two near-fault records belonging to soil class A and B are compared with the EC8 spectral shapes and the ITA08 GMPE. The EC8 spectrum is scaled with the expected peak ground acceleration with 10% probability of exceedance in 50 years. The spectrum designed for rock sites is conservative at high periods, while the observations for class B exceed both short periods (0-0.4s) and intermediate periods (0.8 – 1.5s).

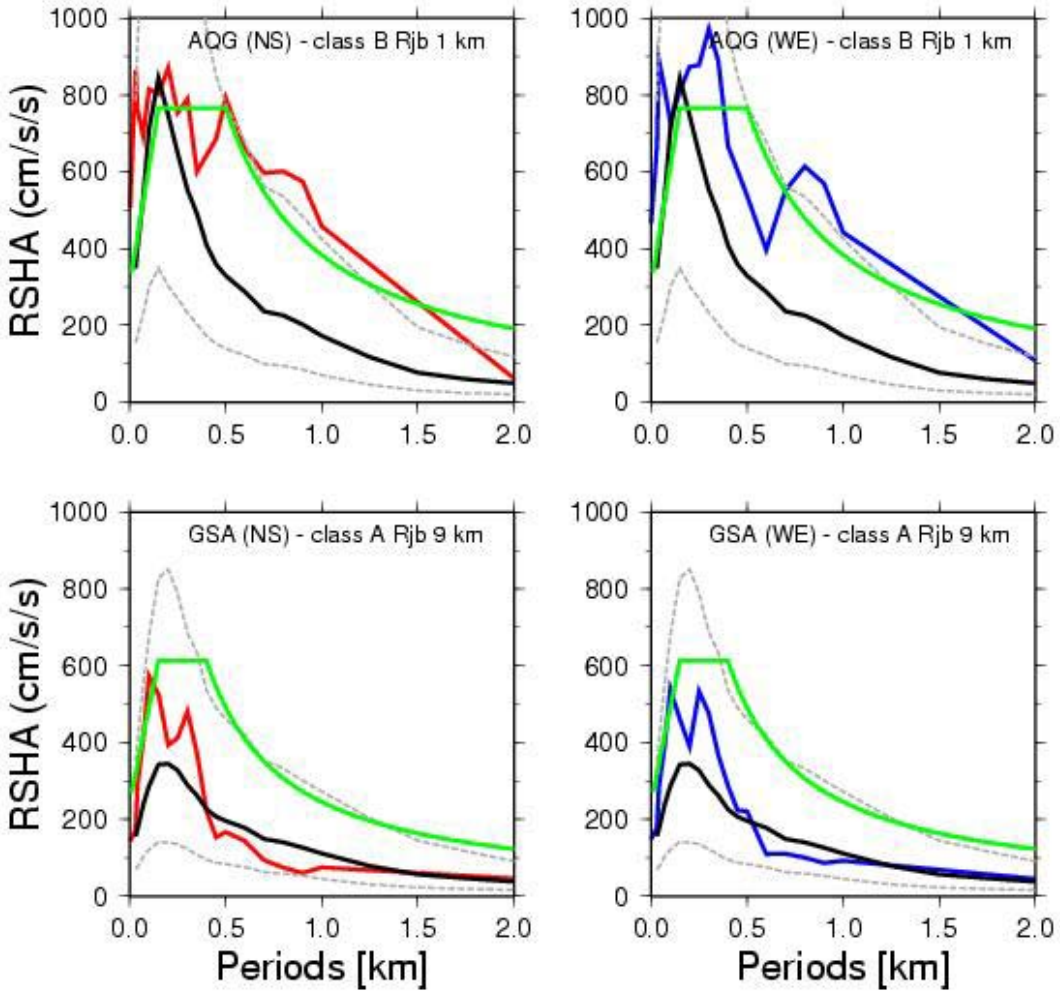

Figure 13 - Comparison between observed spectra and EC8 spectral shapes scaled to the PGA of the national hazard map (0.25 g).

7. Site effects in the upper Aterno valley

A strong motion array, transversal to the upper Aterno valley composed of 7 stations, has been installed by the Italian civil protection, in order to detect the variation of the seismic motion along the valley (Figure 14). For some stations of the array we performed H/V ratio in order to detect the resonance frequency, using the ground motion recorded by the national accelerometric network before 2005. In particular, the site *Valle dell'Aterno centro valle* (AQV), was investigated in detail in the project "Italian strong motion data base in the period 1972-2004 in the framework of the agreement between Istituto Nazionale di Geofisica e Vulcanologia and Department of Civil Protection 2004-2006. A cross-hole test is available for the site shown in Figure 15.

The station Aquilpark (AQK), installed in the L'Aquila town has a remarkable amplification at low frequency (about 0.6 Hz, figure 16c), as also demonstrated by De Luca et al. (2005) using weak motion and ambient noise data. The stations AQV, AQA and AQG installed in the upper Aterno valley have a response at higher frequencies than AQK (2 Hz, 9.5 Hz and a broad amplification range between 2 and 6 Hz, respectively), as shown in Figure 16a-b-d. In Figure 16d is also shown the 1D linear model computed from the shear wave velocity profile in Figure 15.

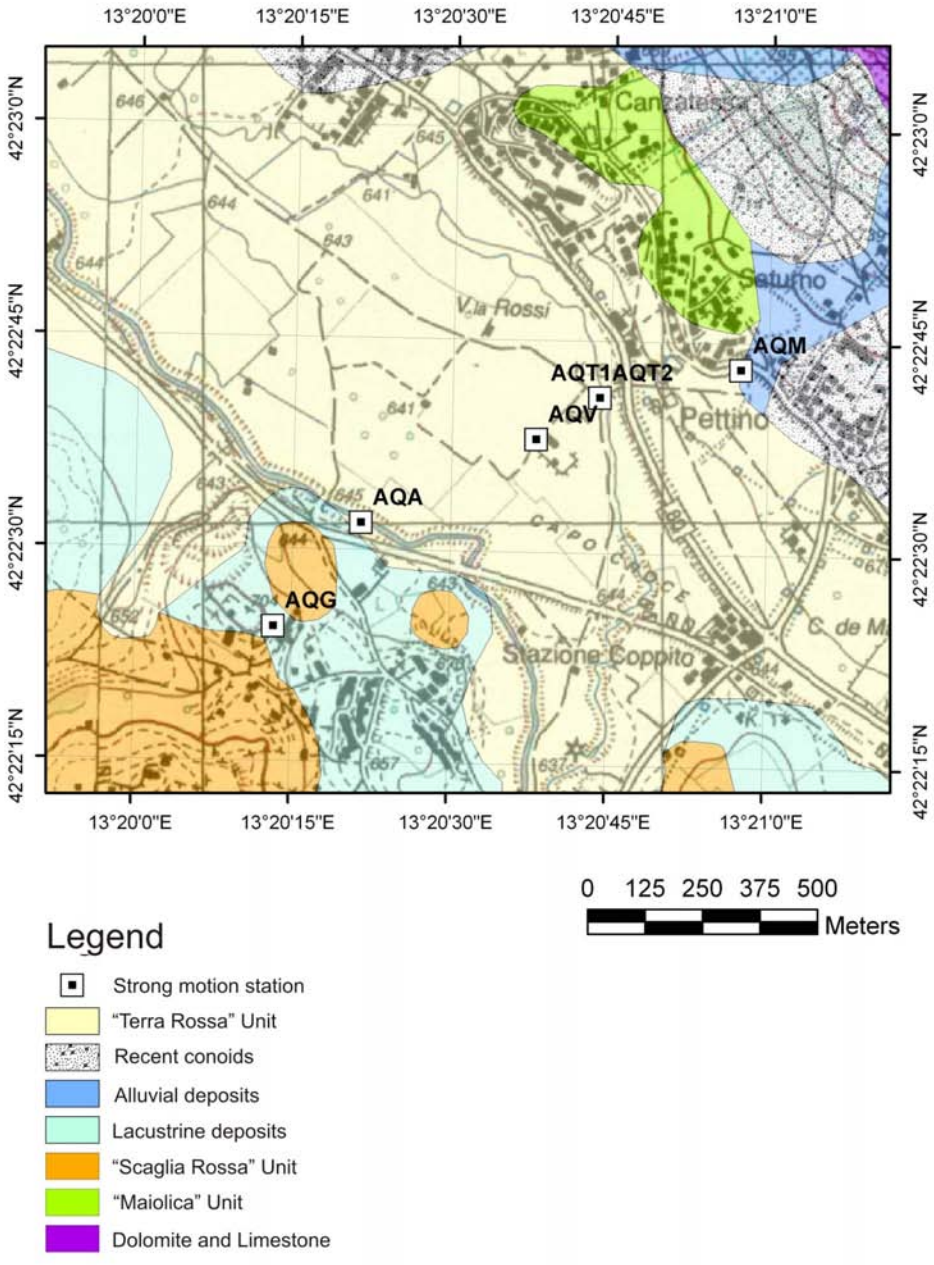

Figure 14 - geologic map of the upper Aterno valley. Squares indicate the array stations.

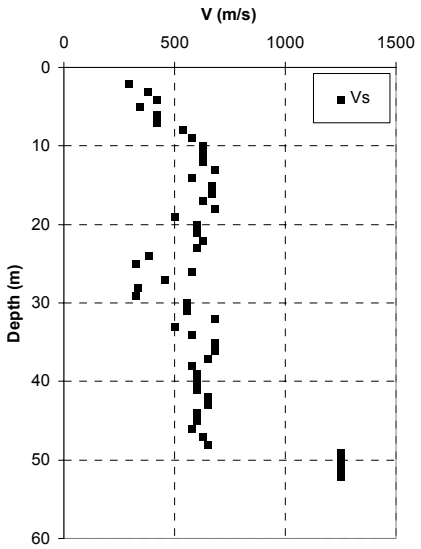

Figure 15 - shear wave velocity profile at AQV (ITACA database http://itaca.mi.ingv.it)

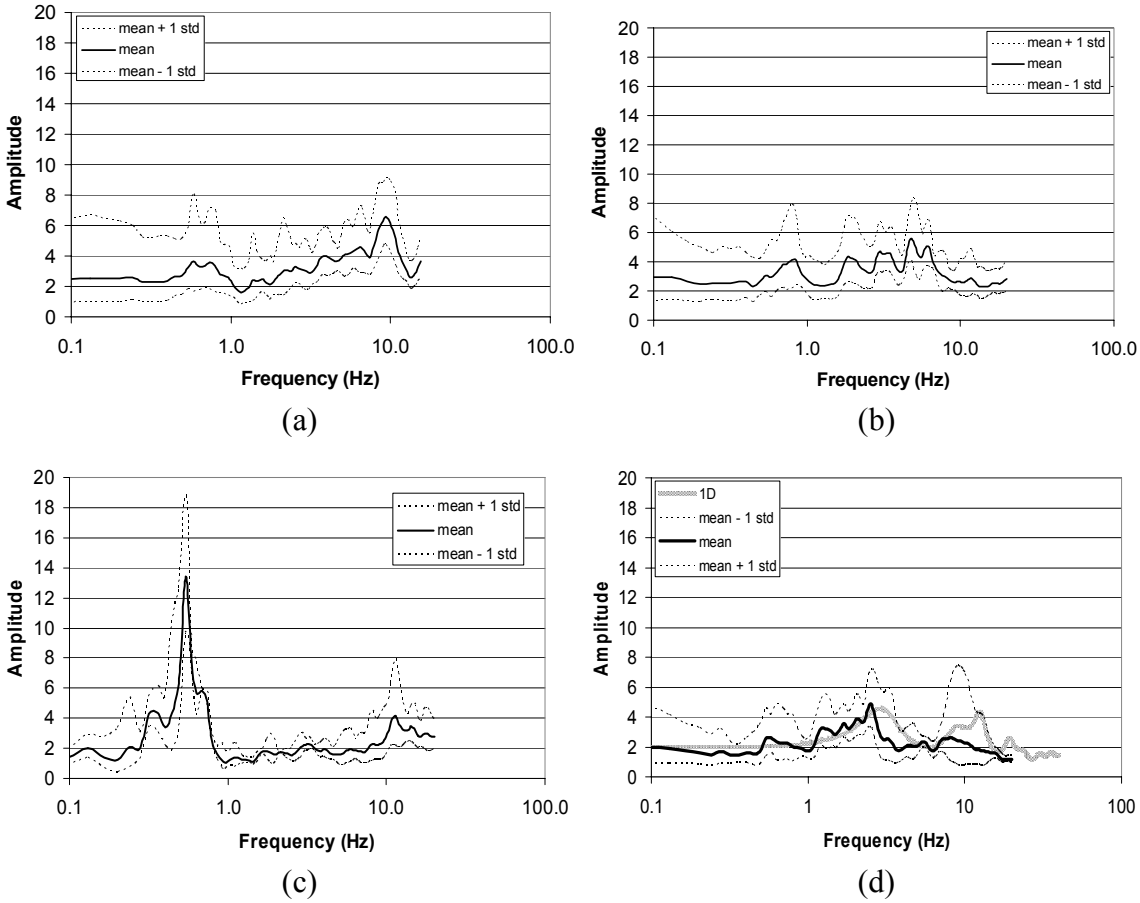

Figure 16 - H/V spectral ratios from strong motion data at a) AQA, b) AQG, c) AQK, d) AQV

References

Akkar S, Bommer JJ (2007) Empirical Prediction Equations for Peak Ground Velocity Derived from Strong-Motion Records from Europe and the Middle East. *Bull Seism Soc Am*., **97**, 511-530.

Ambraseys, N. N., Douglas, J., Sarma, S. K. and P. M. Smit (2005). Equations for the estimation of strong ground motions from shallow crustal earthquakes using data from Europe and Middle East: Horizontal peak ground acceleration and spectral acceleration. *Bull. Earth. Eng.*, **3**, 1-53.

Cauzzi C. and E. Faccioli (2008) Broadband (0.05 to 20 s) prediction of displacement response spectra based on worldwide digital records. *J. Seismol*., **12**, 453-475

Bindi D., L. Luzi, M. Massa, F. Pacor (2008) Horizontal and vertical ground motion prediction equations derived from the Italian Accelerometric Archive (ITACA). *Bull Earth. Eng.*, submitted.

G. De Luca, S. Marcucci, G. Milana, T. Sano' (2005) - Evidence of Low-Frequency Amplification in the City of L'Aquila, Central Italy, through a Multidisciplinary Approach Including Strong- and Weak-Motion Data, Ambient Noise, and Numerical Modeling. *Bull Seism Soc Am*., **95**, 1469 - 1481.

Sabetta F, Pugliese A (1987) Attenuation of peak ground acceleration and velocity from Italian strong motion records. *Bull Seism Soc Am*., **77**, 1491-1513.

Sabetta F, Pugliese A (1996) Estimation of response spectra and simulation of non-stationary earthquake ground motions. *Bull Seism Soc Am*., **86**, 337-352.

Stucchi et alii. (2007). DBMI04, il database delle osservazioni macrosismiche dei terremoti italiani utilizzate per la compilazione del catalogo parametrico CPTI04. http://emidius.mi.ingv.it/DBMI04/. *Quaderni di Geofisica*, **49**, pp.38.